BIOCHEMISTRY
including biophysical chemistry & molecular biology

Article

pubs.acs.org/biochemistry

# Initiation of RNA Synthesis by the Hepatitis C Virus RNA-Dependent RNA Polymerase Is Affected by the Structure of the RNA Template

Stefan Reich,[†] Michael Kovermann,[‡] Hauke Lilie,[§] Paul Knick,[†] René Geissler,[†] Ralph Peter Golbik,*[,†] Jochen Balbach,[‡] and Sven-Erik Behrens*[,†]

[†]Institute of Biochemistry and Biotechnology, Section of Microbial Biotechnology, [‡]Institute of Physics, Section of Biophysics, [§]Institute of Biochemistry and Biotechnology, Section of Technical Biochemistry, Martin Luther University Halle-Wittenberg, D-06120 Halle/Saale, Germany

Supporting Information

**ABSTRACT:** The hepatitis C virus (HCV) RNA-dependent RNA polymerase NS5B is a central enzyme of the intracellular replication of the viral (+)RNA genome. Here, we studied the individual steps of NS5B-catalyzed RNA synthesis by a combination of biophysical methods, including real-time 1D $^1$H NMR spectroscopy. NS5B was found to bind to a nonstructured and a structured RNA template in different modes. Following NTP binding and conversion to the catalysis-competent ternary complex, the polymerase revealed an improved affinity for the template. By monitoring the folding/unfolding of 3′(−)SL by $^1$H NMR, the base pair at the stem's edge was identified as the most stable component of the structure. $^1$H NMR real-time analysis of NS5B-catalyzed RNA synthesis on 3′(−)SL showed that a pronounced lag phase preceded the processive polymerization reaction. The presence of the double-stranded stem with the edge base pair acting as the main energy barrier impaired RNA synthesis catalyzed by NS5B. Our observations suggest a crucial role of RNA-modulating factors in the HCV replication process.

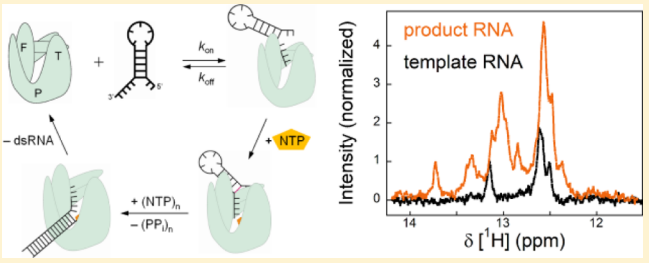


Hepatitis C virus (HCV), a member of the *Flaviviridae* family, is a major causative agent for liver cirrhosis and hepatocellular carcinoma in man.[1] The infection of a host cell by HCV is followed by the release of the about 9.6 kb single-stranded (+)RNA viral genome that is translated and replicated in the cytoplasm.[2] The central enzyme involved in the viral RNA replication process is the RNA-dependent RNA polymerase (RdRp) NS5B.[3,4] As part of an as yet incompletely characterized viral replication complex, the HCV-polymerase initiates RNA polymerization *de novo* and first copies the (+)RNA, generating (−)RNA molecules.[5,6] In a second step, the 3′-end of the (−)RNA serves as an initiation site for the polymerase, which then catalyzes the synthesis of progeny (+)RNAs. The latter step can be easily recapitulated with the purified enzyme and accordingly serves as a suitable model in studies aimed at understanding the mechanisms that underlie the initiation of RNA polymerization on an authentic template (see scheme in Figure 1A).

Generally, the catalytic action of the HCV-polymerase involves a conformational transition from an initiation to an elongation state.[7−12] Several crystal structures were solved, and the HCV-polymerase was shown to display a classic right-handed topology.[13−18] Accordingly, the palm domain contains the residues responsible for catalysis and NTP binding, whereas the finger and thumb domains are in tight contact in the initiation-competent "enclosed form" of the polymerase. The RNA template is assumed to enter the polymerase through a hydrophilic groove in the finger's subdomain.[19] A $\beta$-hairpin loop in the thumb domain located close to the active site is supposed to function in positioning the 3′-end of the RNA template.[17] Conformational changes of the HCV-polymerase such as a rotation of the thumb domain or a reorientation of the C-terminus were suggested to accommodate the formation of the double-stranded RNA product.[14,17,20−24] The HCV-polymerase is expected to feature as yet undisclosed conformational regulatory properties during its activity on an authentic RNA template.[25] In the present study, we applied a novel combination of biophysical methods and one-dimensional, real-time proton nuclear magnetic resonance (1D $^1$H NMR) spectroscopy[26,27] to the HCV-polymerase while operating on an RNA template that corresponds to the (−)RNA 3′-end. Thus, we could (i) elucidate the local stability and thermodynamics of the RNA template, (ii) follow the thermodynamics and kinetics of binary and ternary complex formation, which were shown to be associated with conformational changes of the polymerase, and (iii) continuously monitor product formation. The obtained NMR data confirmed earlier indications that the viral polymerase acts in a processive manner. Most interestingly, with the applied partially double-stranded RNA template, the activity of NS5B

**Received:** May 30, 2014
**Revised:** September 16, 2014
**Published:** October 13, 2014

   dx.doi.org/10.1021/bi5006656 | *Biochemistry* 2014, 53, 7002−7012

was substantially delayed. The study hence excluded NS5B acting as an RNA helicase and emphasized the need for further RNA-modulating factors that assist the RdRp during the viral replication process.

## MATERIALS AND METHODS

**Preparation of the HCV-Polymerase.** The gene coding for HCV-polymerase NS5B (genotype 2a, subtype JFH-1) containing a deletion of 21 amino acids at the C-terminus was cloned into the pET SUMO vector and expressed in *Escherichia coli* strain BL21 (DE3) star. Biomass production, gene expression, and purification of HCV-polymerase were carried out as described[28] with minor modifications (see Supporting Information Materials and Methods). Purified HCV-polymerase was dialyzed against 50 mM HEPES/NaOH, 20% (v/v) glycerol, 6.5 mM $MgCl_2$, 2 mM TCEP, pH 7.5 (referred to as assay buffer), centrifuged, and stored at −80 °C. Protein concentration was determined by measuring the absorbance at 280 nm using $\varepsilon_{280}$ = 85 260 $M^{-1}$ $cm^{-1}$.

**Nucleotides and Oligonucleotides.** NTP(s) used for the RNA-dependent RNA polymerization reaction were purchased from Thermo. NTPs used to quantify interactions with the HCV-polymerase by circular dichroism spectroscopy were purchased from Sigma-Aldrich. The oligonucleotides 5′-CUAAGAUGCUCGCUGC-3′ (single-stranded RNA) and 5′-UCGCCCCUAUUAG GGGCAGGU-3′ (3′(−)SL RNA) as well as the 5′-FAM-EX-5-labeled RNAs were purchased from IBA (Göttingen, Germany). The concentrations of unlabeled oligonucleotides were determined by absorbance at 260 nm using the extinction coefficients $\varepsilon_{260}$ = 148 600 $M^{-1}$ $cm^{-1}$ (ssRNA) and $\varepsilon_{260}$ = 200 400 $M^{-1}$ $cm^{-1}$ (3′(−)SL RNA). The concentration of the 5′-FAM fluorescently labeled template RNA was determined from the absorbance at 260 nm using the extinction coefficient $\varepsilon_{260}$ = 148 600 $M^{-1}$ $cm^{-1}$.

**Circular Dichroism Spectroscopy.** Far-UV circular dichroism was applied to monitor the binding of NTPs to HCV-polymerase (nucleotide complex formation) as described previously.[28] Measurements were performed in assay buffer using an enzyme concentration of 20 $\mu$M.

**Fluorescence Spectroscopy.** HCV-polymerase NS5B (genotype 2a, subtype JFH-1) was added to 50 nM 5′-FAM-EX-5-labeled RNA in assay buffer supplemented with NaCl at the concentrations indicated. Fluorescence changes were monitored on a Fluoromax-4 Spectrofluorometer (Jobin Yvon, France) at 22.5 °C unless otherwise stated. After attaining equilibrium, the signal amplitudes of the FAM-probed RNAs were measured (excitation at 491 nm, emission at 515 nm, slit widths 0.2 and 5 nm) and corrected for the volume change. Fluorescence intensities relative to the starting fluorescence were plotted against the protein concentration. Fitting the binding isotherms according to eq 1 with the program KaleidaGraph (Synergy Software) yielded the $K_D$ values of the interaction of HCV-polymerase with the labeled RNA.

$$\Delta F = 1 - \frac{(m + n + K_D) - \sqrt{(m + n + K_D)^2 - 4mn}}{2m} \quad (1)$$

where $\Delta F$ is the change of normalized fluorescence, $m$ is the concentration of the 5′-FAM-EX-5-labeled template RNA, $n$ is the concentration of NS5BΔ21, and $K_D$ is the equilibrium constant between RNA and e.g. HCV-NS5B. The equilibrium constants of the binary complexes in dependence on the salt concentration were determined and analyzed according to a linear free energy relationship using eq 2.

$$\Delta G^0 = -RT \ln K_a \quad (2)$$

$$\Delta G^0 = \Delta G_b^0 - m[\mathrm{NaCl}]$$

$$\ln K_a = \frac{m}{RT}[\mathrm{NaCl}] - \frac{\Delta G_b^0}{RT}$$

where $\Delta G^0$ is the difference in free energy at equilibrium, $\Delta G_b^0$ is the difference in free energy at equilibrium at ionic strength of the buffer, $R$ is the gas constant, $T$ is the temperature (K), $m$ is the correlation coefficient in the linear free energy relationship, and $K_a$ is the association constant between the RNA and HCV-polymerase. The equilibrium constants of HCV-polymerase and labeled RNAs were determined in the assay buffer supplemented with 150 mM NaCl at different temperatures. Data was analyzed according to van't Hoff (eq 3), which revealed the thermodynamic parameters for binary complex formation.

$$\Delta G^0 = -RT \ln K_a \quad (3)$$

$$\Delta G^0 = \Delta H^0 - T\Delta S^0$$

$$\ln K_a = -\frac{\Delta H^0}{RT} + \frac{\Delta S^0}{R}$$

where $\Delta G^0$ is the difference in free energy at equilibrium, $\Delta H^0$ is the difference in free enthalpy at equilibrium, $\Delta S^0$ is the difference in free entropy at equilibrium, $R$ is the gas constant, $T$ is the temperature (K), and $K_a$ is the association constant between the RNA and HCV-polymerase. Fast kinetics of association and dissociation of RNA and HCV-polymerase were performed as described previously.[28] Data was evaluated according to eqs 4 and 5.

$$\Delta F = -v\, e^{-k_v' t} - x\, e^{-k_x' t} - y\, e^{-k_y' t} - z\, e^{-k_z' t} + n \quad (4)$$

$$k_v' = k_{on}[\mathrm{RNA}] + k_{off} \quad (5)$$

where $\Delta F$ is the total change of relative fluorescence amplitude; $v$, $x$, $y$, and $z$ are the signal amplitudes of the respective phases; $k_v'$, $k_x'$, $k_y'$, and $k_z'$ are the first-order rate constants of the respective phases; $t$ is the time; $n$ is the relative fluorescence intensity at the end point of the reaction (offset); $k_{on}$ is the rate constant of substrate association (bimolecular reaction); and $k_{off}$ is the rate constant of substrate dissociation (monomolecular reaction). All thermodynamic and kinetic measurements were performed at least in duplicate. Errors of the parameters obtained from the fitting routine were in the range of 10%.

**NMR Spectroscopy.** All 1D $^1$H NMR spectra were recorded in 50 mM HEPES/NaOH, 200 mM NaCl, 6.5 mM $MgCl_2$, 1 mM TCEP, pH 7.5, at 295.6 K, containing 10% (v/v) $D_2O$ and 5% (v/v) deuterated glycerol. Data was acquired on a Bruker Avance III 600 MHz spectrometer equipped with a room temperature probe or on an Avance III 800 MHz spectrometer equipped with a cryoprobe. Water suppression was achieved by usage of the double pulsed field gradient spin echo approach.[44] Spectra were processed using TopSpin 2.1. Five hertz exponential line broadening and polynomial baseline correction were manually applied before integration of the spectra. Spectra monitoring the RNA-dependent RNA


dx.doi.org/10.1021/bi5006656 | *Biochemistry* 2014, 53, 7002−7012

polymerization reactions were recorded using 30 $\mu$M HCV-polymerase and 30 $\mu$M 3′(−)SL RNA either with or without 0.5 mM nucleotides. Spectra accumulated for a time period of 21 h were normalized to the spectra accumulated for a time period of 8 h by the factor 0.4 ($^8/_{21}$). Integrals of the 1D $^1$H NMR spectra in the region of interest were plotted against the reaction time. The reaction times indicated correspond to the beginning of recording the respective NMR spectra plus half of the time resolution of each spectrum. Two-dimensional $^1$H−$^1$H NMR NOESY spectra to assign the imino proton NMR signals were acquired at a temperature of 295.6 K using mixing times of $t_m$ = 120 and 250 ms. Spectra were recorded with spectral widths of 20.01 ppm in both dimensions. The $^1$H carrier frequency was set to 4.7 ppm. 1024 increments were recorded in the indirect dimension, and 8192 points in the direct dimension. Each increment was recorded with 160 scans. Water suppression was achieved using the double pulsed field gradient spin echo approach.[44]

**Thermodynamic Stability of the Secondary Structure of the 3′(−)SL RNA.** The signal intensity changes of the imino protons in the 1D $^1$H NMR spectrum of 100 $\mu$M 3′(−)SL RNA were recorded at 278, 286, 294, 302, 310, 318, 326, 334, 342, 350, and 358 K. The integrated signals, correlating to the double-stranded character of the respective base pairs, were analyzed according to a two-state folding mechanism (eq 6), yielding the thermodynamic parameters of the secondary structure.

$$\Delta G^0_T = \Delta H^0_{T_m}\left(1 - \frac{T}{T_m}\right) - \Delta C_p\left[T_m - T + T\left(1 - \frac{T}{T_m}\right)\right] \quad (6)$$

$$\Delta G^0_{T_m} = \Delta H^0_{T_m} - T\Delta S^0_{T_m} = 0$$

$$\Delta S^0_{T_m} = \frac{\Delta H^0_{T_m}}{T_m}$$

$$X = \frac{n_N + n_U\, e^z}{1 + e^z}$$

$$z = \frac{\Delta H^0_{T_m}\left(1 - \frac{T}{T_m}\right) - \Delta C_p\left[T_m - T + T\left(1 - \frac{T}{T_m}\right)\right]}{RT}$$

where $\Delta G^0_T$ is the difference in free energy at equilibrium and temperature $T_m$ (K), $\Delta H^0_{T_m}$ is the difference in free enthalpie at equilibrium and temperature $T_m$ (K), $\Delta S^0_{T_m}$ is the difference in free entropy at equilibrium and temperature $T$ (K), $\Delta C_p$ is the change in heat capacity during folding/unfolding, $T_m$ is the temperature at the transition midpoint, $X$ is the signal intensity change of the imino proton signal in the 1D $^1$H NMR spectrum, $n_N$ is the signal intensity of the native imino proton signal in the 1D $^1$H NMR spectrum, and $n_U$ is the signal intensity of the unfolded imino proton signal in the 1D $^1$H NMR spectrum.

## RESULTS

**Binary Complex Formation: Binding of the RNA Template by the Polymerase.** RNA synthesis catalyzed by the HCV-polymerase is a two-substrate reaction (Figure 1A). The first half-reaction involves the binding of the RNA template by the active site of the enzyme. To evaluate the binding behavior of the HCV-polymerase with differently

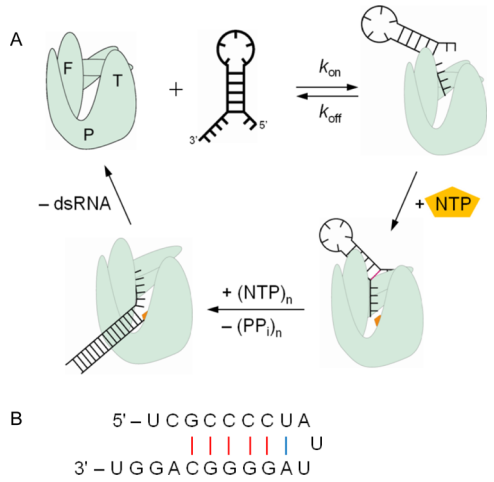


**Figure 1.** RNA synthesis catalyzed by the HCV-polymerase on the structured 3′(−)SL RNA template. (A) The HCV-polymerase NS5B is schematically depicted with thumb (T), palm (P), and finger (F) domains. The 3′(−)SL RNA template forms a stem-loop structure; the inset provides the secondary structures that were determined by NMR (see also Figures 4 and 5 and Table 3). For the synthesis of progeny (+)RNA molecules, the HCV-polymerase binds in a first half-reaction (binary complex formation). The interaction with NTPs (as indicated) results in the formation of the catalysis-competent ternary complex. Our data suggest that RNA secondary structures of the template have to be resolved to accomplish double-stranded RNA product formation and release (second half-reaction). (B) Schematic presentation of the primary structure of the 3′(−)SL RNA template. Two possible structures of the stem-loop were derived by the program mfold.[45]

structured RNAs, we applied a previously established assay[28] utilizing a purified HCV-polymerase (HCV genotype 2a, subtype JFH-1) and two fluorescently labeled RNA templates, i.e., (1) a randomly composed 16 nt single-stranded oligonucleotide (ssRNA) and (2) a 21 nt oligonucleotide that forms a stable stem-loop structure (Figure 1B). The latter RNA, termed here as 3′(−)SL, corresponds to the immediate 3′-end of the HCV (−)RNA. It was used to mimic the initiation of the second step of the viral RNA replication process, the synthesis of progeny (+)RNA. Under physiological conditions, the HCV-polymerase revealed the highest affinity to the random ssRNA template (Figure 2A and Table 1). Elevation of the ionic strength by NaCl perturbed the polymerase−RNA association and decreased the affinity following a linear free energy relationship (LFER). The dependence on the ionic conditions was less pronounced during binding of the HCV-polymerase to the 3′(−)SL RNA. This suggested that the formation of the binary complex with 3′(−)SL followed a different mode involving, for example, additional nonionic contributions that were not screened by salt.

To dissect the GIBBS free energy of binding ($\Delta G$) by its enthalpic ($\Delta H$) and entropic ($\Delta S$) contributions, the temperature dependence of the respective equilibrium constants was measured and analyzed according to the van't Hoff approximation (Figure 2B and Table 1). Binary complex formation of the HCV-polymerase with ssRNA resulted in a $\Delta H^0 \approx 0$. In contrast, an endothermic reaction ($\Delta H^0 > 0$) was observed for binding of the 3′(−)SL RNA. However, with this RNA, the positive and unfavorable binding enthalpy was compensated by a significant change in entropy. Thus, in comparison to the association of the HCV-polymerase with the


dx.doi.org/10.1021/bi5006656 | Biochemistry 2014, 53, 7002−7012

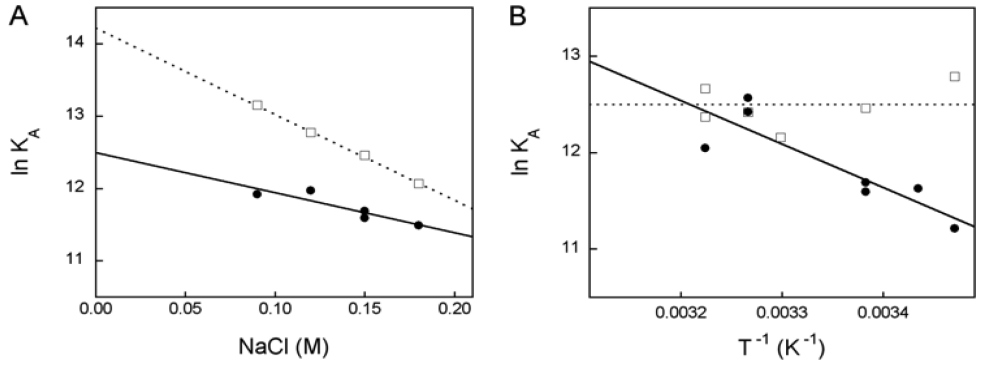


**Figure 2.** Characterization of the binding of the HCV-polymerase to different RNA templates. Association constants of fluorescently labeled RNAs and the HCV-polymerase were determined as described in the Materials and Methods. (A) Binding of the HCV-polymerase to ssRNA (white squares) and to the 3′(−)SL RNA (black circles) was determined as a function of the concentration of NaCl at 22.5 °C. The affinity constants were analyzed according to a linear free energy relationship[46,47] with NaCl perturbing the binary complex formation. (B) Association constants of the HCV-polymerase and ssRNA (white squares) and the 3′(−)SL RNA (black circles) were determined as a function of temperature at 0.15 M NaCl and analyzed according to the van't Hoff approximation. The respective thermodynamic parameters are summarized in Table 1.

**Table 1. Parameters of RNA Binding to the HCV-Polymerase**

| RNA template | $m$ (kJ mol$^{-1}$ M$^{-1}$)[a] | $\Delta G$ (kJ mol$^{-1}$)[b] | $\Delta H$ (kJ mol$^{-1}$)[b] | $-T\Delta S$ (kJ mol$^{-1}$)[b] |
|---|---|---|---|---|
| ssRNA | −29.3 ± 0.9 | −30.6 ± 0.1 | ≈0 | −30.7 ± 0.2 |
| 3′(−)SL RNA | −13.6 ± 3.7 | −28.7 ± 0.5 | +37.4 ± 9.3 | −66.3 ± 9.2 |

[a]Perturbation of the polymerase−RNA interaction by NaCl at 22.5 °C (slope of the LFER). [b]Thermodynamic parameters of polymerase−RNA interaction at an ionic strength of 0.192 M (0.15 M NaCl) and at 22.5 °C.

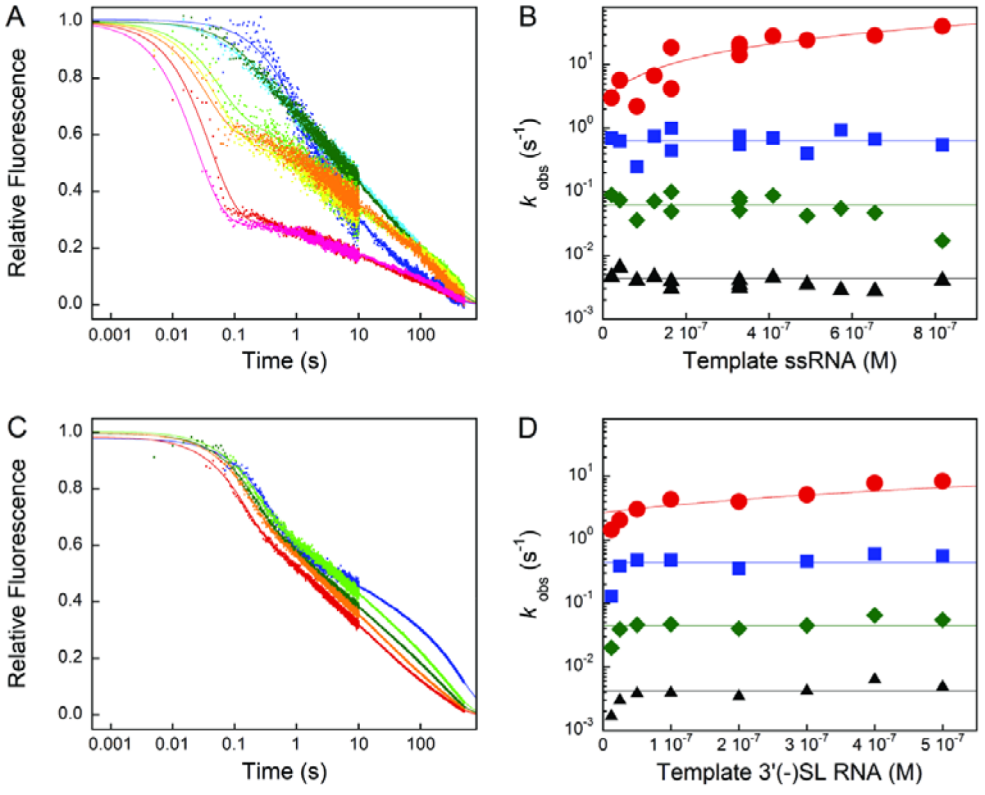


**Figure 3.** Binding kinetics of the HCV-polymerase to short RNAs (binary complex formation). The kinetics of binary complex formation was measured using fluorescently labeled RNAs. The binding process of single-stranded RNA (16 nucleotides) (A) was recorded at template concentrations of 21 nM (dark blue), 124 nM (light blue), 164 nM (dark green), 185 nM (lime), 329 nM (yellow), 410 nM (orange), 492 nM (red), and 817 nM (pink). Binding the native 3′(−)SL RNA (21 nucleotides) (C) was recorded at template concentrations of 12.5 nM (dark blue), 100 nM (dark green), 200 nM (lime), 300 nM (orange), and 500 nM (red). The protein concentration was 270 nM. Complex formation proceeded at least via three intermediates; accordingly, the kinetics was fitted according to quadruple-exponential first-order reactions (B, D). The observed rate constants were plotted against the respective RNA concentration and yielded a second-order rate constant and three intramolecular first-order rate constants that are summarized in Table 2.


dx.doi.org/10.1021/bi5006656 | *Biochemistry* 2014, 53, 7002−7012

Table 2. Rate Constants of the Binding Process of RNA Templates to HCV-Polymerase[a]

| RNA template | $k_{on}^{1}$ ($\mu M^{-1}$ $s^{-1}$) | $k_{off}^{1}$ ($s^{-1}$) | $k_1'$ $10^{-1}$ ($s^{-1}$) | $k_2'$ $10^{-2}$ ($s^{-1}$) | $k_3'$ $10^{-3}$ ($s^{-1}$) |
|---|---|---|---|---|---|
| ssRNA | 45.9 ± 5.3 | 2.7 ± 2.0 | 6.4 ± 0.5 | 6.2 ± 0.6 | 4.3 ± 0.3 |
| 3′(−)SL RNA | 7.9 ± 1.9 | 2.7 ± 0.7 | 4.4 ± 0.5 | 4.5 ± 0.4 | 4.2 ± 0.5 |

[a]Kinetics was fitted according to quadruple-exponential first-order reactions. Second-order rate constants $k_{on}^{1}$ and first-order rate constants $k_{off}^{1}$ were derived from the concentration dependence of $k_v'$. Experiments were performed as described in the Materials and Methods.

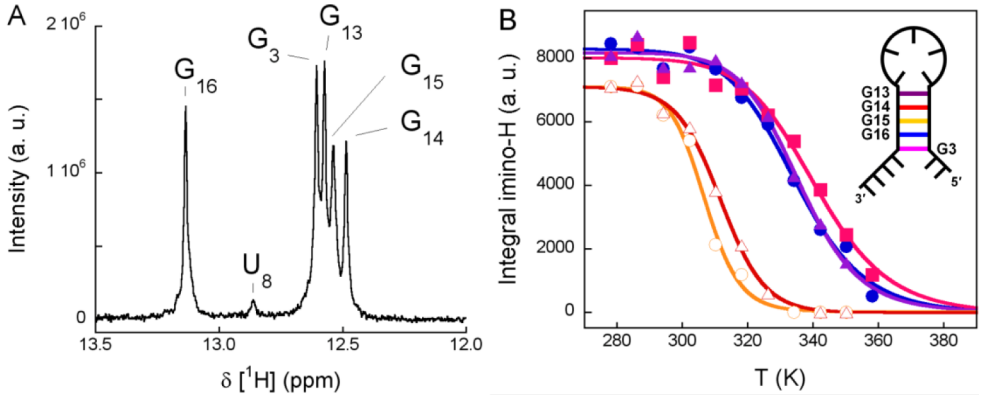


**Figure 4.** Structural analysis and thermodynamic stability of the stem-loop formed by a 21 nt RNA oligonucleotide corresponding to the 3′-end of the HCV (−)RNA. (A) One-dimensional $^1$H NMR spectrum of the 3′(−)SL RNA. The RNA displays 5 prominent base pairs that form the stem. The spectral region that is sensitive for double-stranded RNA is shown. Each signal corresponds to the respective imino proton that contributes to hydrogen bonding of one canonical base pair, as indicated. Assignment of the individual signals was performed by a NOESY spectrum and by considering some RNA variants (see Figure 5). (B) The thermodynamic stability of the stem structure of the 3′(−)SL RNA was determined from thermal unfolding transitions monitored by 1D $^1$H NMR spectroscopy that are sensitive to individual base pairing within the stem. Integrated signal intensities of the respective imino protons were analyzed according to a two-state folding−unfolding mechanism ($G_3$−$C_{17}$, filled square; $G_{16}$−$C_4$, filled circle; $G_{15}$−$C_5$, open circle; $G_{14}$−$C_6$, open triangle; $G_{13}$−$C_7$, filled triangle). The thermodynamic parameters that derived from fitting the transition curves are summarized in Table 3. The secondary structure of the RNA is schematically shown in the inset.

ssRNA, the favorable entropic contributions (population of microstates) along with the binding of the enzyme to the structured 3′(−)SL RNA increased by a factor of 2. With both, the ssRNA and the 3′(−)SL RNA, the interaction of the polymerase accordingly turned out to be entropically driven, which may be related to the conformational freedom of the binary complex. In the case of the native 3′(−)SL RNA, the increased entropic change was assumed to result from a partial disbanding of the stem structure or from a specific rearrangement of the polymerase's conformation on binding.

Kinetically, the RNA binding by the HCV-polymerase proceeded along defined intermediates. Both RNA templates were shown to interact with the HCV-polymerase via initial Michaelis-complex formation and some subsequent intramolecular reactions (Figure 3 and Table 2). In analogy to earlier findings,[28] four phases of template binding were resolved, which could be differentiated by their rate constant and by the amplitude of quenching of the fluorescence emission of the labeled RNA. The fastest process depended on the RNA concentration; accordingly, we assigned this phase to the initial complex formation as a second-order reaction. The three slower processes did not depend on the RNA concentrations and were attributed to intramolecular rearrangements.[28] The kinetics of the interaction between the HCV-polymerase and the two RNA templates significantly differed only in the fastest process, corresponding to the second-order rate constant $k_{on}$ of association. Here, the native 3′(−)SL RNA template was observed to bind 6-fold slower than the random ssRNA. No significant differences were observed for the three slower monomolecular reactions and the first-order dissociation rate constant $k_{off}$. This indicated that the intramolecular substrate positioning and release by the polymerase mostly occurred independently of the RNA moiety.

**Structure and Thermodynamics of the 3′(−)SL RNA.** To analyze the thermodynamic stability of the 3′(−)SL RNA and its conformational changes during substrate turnover in the enzymatic reaction, we applied 1D $^1$H NMR spectroscopy. For this purpose, the NMR resonances of the imino protons of the nucleobases were utilized;[29] these were generally well-resolved in the proton spectra (Figure 4) and easily assignable to the respective nucleotide base (Figure 5). Base-paired imino protons are able to form hydrogen bonds and are discernible because the exchange rate with the solvent is strongly reduced. Their signal intensity reports on each single canonical base pairing. Along this line, the secondary structure of the native RNA was first confirmed to predominantly consist of a stem-loop with 5 base pairs composed of $G_3C_4C_5C_6C_7$ and $G_{13}G_{14}G_{15}G_{16}C_{17}$ and a penta-loop (Figure 4). An additional signal at 12.85 ppm in the spectrum accounted for a less stable sixth U−A bp ($U_8$ and $A_{12}$) of an underrepresented stem-loop with a triple-loop structure. Both RNA species were in equilibrium under the chosen conditions. Subsequent measurements of the thermodynamic stability of these structures in the 3′(−)SL RNA revealed a cooperative transition pattern during temperature-induced unfolding (Figure 4B and Table 3). Interestingly, the $G_3$−$C_{17}$ bp at the edge of the stem turned out to be most stable and showed a transition temperature ($T_m$) of 341 K followed by $C_7$−$G_{13}$ (336 K) and $C_4$−$G_{16}$ (335 K). $C_5$−$G_{15}$ (307 K) and $C_6$−$G_{14}$ (312 K) were less stable and remained unpaired for a significant number of molecules, even at room temperature.

**Ternary Complex Formation: Binding of NTPs and RNA by the Polymerase.** During the polymerization process,


dx.doi.org/10.1021/bi5006656 | Biochemistry 2014, 53, 7002−7012

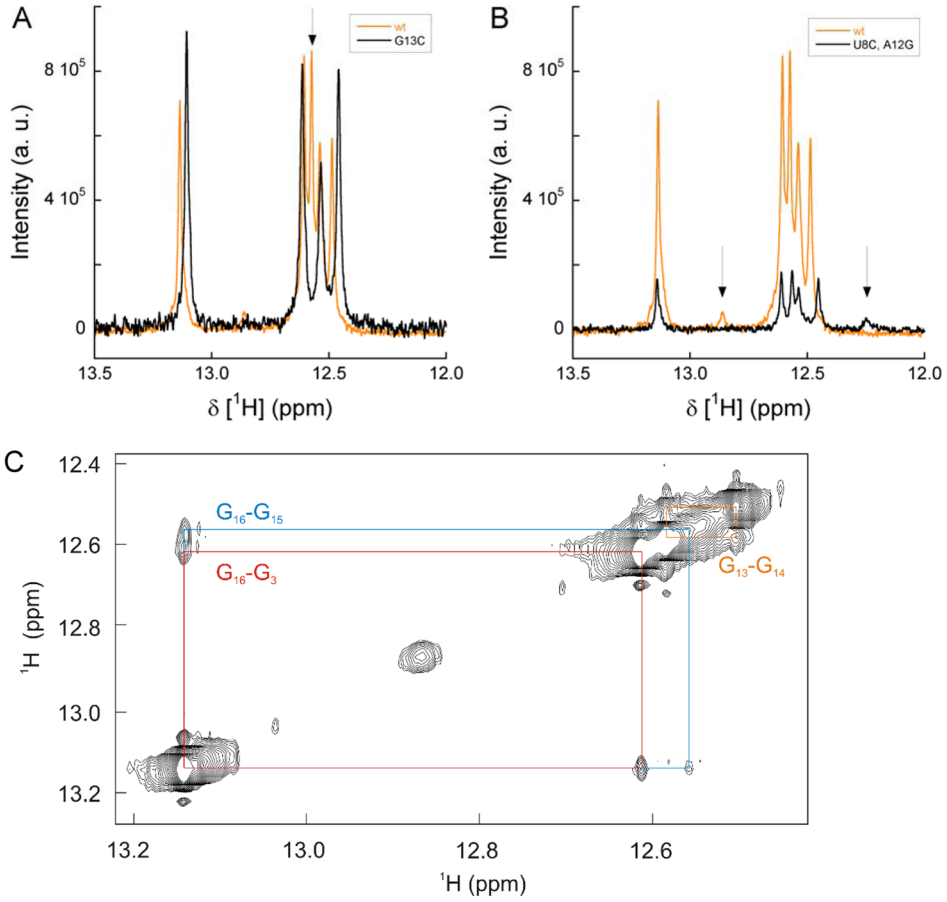


**Figure 5.** Assignment of $^1$H NMR signals to double-stranded base pairs that form the 3′(−)SL RNA secondary structure. The 3′(−)SL RNA displays 5 distinct major imino proton signals in the $^1$H NMR spectrum that correspond to a stem-loop RNA secondary structure comprising a 5 base-paired stem, a penta-loop, and 4 and 2 nucleotide single-stranded parts at the 3′- and 5′-ends, respectively. (A) A spectrum of the wild-type 3′(−)SL RNA was compared with the spectrum of a 3′(−)SL RNA mutant G13C, which features only 4 prominent base pairs. This enabled the assignment of the imino proton signal of $G_{13}$, as indicated by the arrow. (B) An alternative stem-loop structure with an additional sixth base pair, $U_8$–$A_{12}$, resulting in a conformation consisting of a 6 base-paired double-stranded stem and a triple-loop, is less populated in solution. This was shown by substitution of the wild-type $U_8$–$A_{12}$ by $C_8$–$G_{12}$, which resulted in a new imino proton signal in the $^1$H NMR spectrum at higher field, as indicated by the arrows. (C) Two-dimensional $^1$H–$^1$H NOESY spectrum of 1 mM 3′(−)SL RNA was recorded, yielding intramolecular imino–imino NOE signals. Depicted are the following NOE cross peaks: $G_{16}$–$G_{15}$, turquoise; $G_{16}$–$G_3$, red; $G_{13}$–$G_{14}$, ocher.

**Table 3. Thermodynamic Parameters of Unfolding of the 3′(−)SL RNA[a]**

| base pair | $\Delta H^0_{T_m}$ (kJ mol$^{-1}$) | $\Delta S^0_{T_m}$ (kJ mol$^{-1}$ K$^{-1}$) | $T_m$ (K) | $\Delta C_p$ (kJ K$^{-1}$ mol$^{-1}$) | $\Delta G^0_{296K}$ (kJ mol$^{-1}$) |
|---|---|---|---|---|---|
| $G_3$ | 88 | 0.26 | 340.8 ± 1.4 | 0.059 | 11.3 |
| $G_{16}$ | 88 | 0.26 | 334.6 ± 1.0 | 0.063 | 10.1 |
| $G_{15}$ | 147 | 0.48 | 306.9 ± 0.7 | 0.113 | 5.0 |
| $G_{14}$ | 118 | 0.38 | 311.7 ± 0.5 | 0.084 | 4.2 |
| $G_{13}$ | 101 | 0.30 | 335.8 ± 0.8 | 0.067 | 11.7 |

[a]Thermodynamic parameters were derived from fitting the thermal unfolding transitions (change of the corresponding integral signal intensities in the $^1$H NMR spectrum) according to a two-state folding model. Errors of the thermodynamic parameters obtained from the fitting routine were in the range of about 20–30%.

the viral RdRp catalyzes RNA synthesis in a nucleotidyl-transfer reaction. Thus, besides binding of the RNA template, the enzyme also associates nucleotides in a second half-reaction. First, we applied UV circular dichroism at the negative local extremum at 241 nm to measure the formation of polymerase–NTP complexes, (Supporting Information Figure S1). The obtained data revealed dissociation constants in a low micromolar range of the respective NTPs as well as a positive cooperativity, which was indicated by a Hill coefficient of ∼1.5 (summarized in Table 4). In the absence of template RNA, two nucleotide molecules associated with the polymerase (see Discussion). In a second approach, the initiation of binary complex formation of the HCV-polymerase with the 3′(−)SL RNA was monitored by 1D $^1$H NMR spectroscopy. The data revealed an overall line-broadening of the imino proton signals in the substrate part of the spectrum. This was explained by an equilibrium formed between the unbound nucleic acid, the signals of which remained detectable, and the high molecular


dx.doi.org/10.1021/bi5006656 | Biochemistry 2014, 53, 7002–7012

Table 4. Binding Parameters of NTP to HCV-Polymerase[a]

| nucleotide | $K_D$ (mM) | $K_S$ (mM$^n$) | Hill-coefficient $n$ |
|---|---|---|---|
| ATP | 0.056 ± 0.001 | 0.011 ± 0.002 | 1.55 ± 0.06 |
| CTP | 0.058 ± 0.002 | 0.012 ± 0.002 | 1.56 ± 0.06 |
| GTP | 0.044 ± 0.002 | 0.009 ± 0.002 | 1.53 ± 0.07 |
| UTP | 0.101 ± 0.002 | 0.038 ± 0.004 | 1.42 ± 0.04 |

[a]NTP binding was measured by circular dichroism change of the HCV-polymerase; parameters were determined by fitting the binding isotherms according to a cooperative binding mode.

weight complex where the RNA-related signals disappeared due to the proton's restricted tumbling motion. To further explore the impact of NTP binding on the binary complex consisting of the HCV-polymerase and the 3′(−)SL RNA template, we again applied time-resolved 1D $^1$H NMR. Interestingly, the addition of NTPs led to an intensity loss of the RNA template's imino proton signals (Figure 6A,B), which indicated a decrease in the concentration of unbound RNA and an increase in the amount of RNA that bound to the polymerase. Hence, the formation of the binary complex increased the affinity of the HCV-polymerase for the RNA template ($K_M < K_D$), leading to the catalysis-competent ternary complex.

**RNA Polymerization Monitored by Real-Time 1D $^1$H NMR Spectroscopy.** Generally, the incorporation of nucleotides by RNA polymerases proceeds by complementary base pairing. To monitor product formation with the 3′(−)SL RNA template directly, we established a time-resolved 1D $^1$H NMR approach, which analyzed the set of imino proton signals of the substrate and product RNAs. The experimental setup was such that a nearly single turnover reaction was investigated. Considering the previously determined binding parameters of all substrates, this was enabled by a minimum of 66% turnover in the first polymerization round. The reaction was followed by spectra recording in 8 and 21 h increments, respectively. Interestingly, during the initial ca. 20 h, the signal profile remained essentially constant and revealed a lag phase where no release of double-stranded product was detectable (Figure 6A,B). We interpreted this finding such that this phase reflects a rearrangement of the enzyme-bound substrate structure that is susceptible to product formation (see Discussion). Within the subsequent ca. 5 h, a set of defined imino proton signals appeared in the 1D $^1$H NMR spectrum that corresponded to newly developed base pairs. The spectra were normalized by setting the signal intensity of the discrete imino proton NMR signal at 13.75 ppm to correspond to 1 bp (marked with an asterisk in Figure 6C). Thus, with the polymerization product, integrated peaks corresponding to 21 bp were detectable in total, indicating that a (+)RNA molecule was synthesized that was full-length complementary to the original 3′(−)SL template. This notion was confirmed when we compared the NMR signals of the polymerization product with those of a chemically synthesized 21 bp dsRNA (Figure 6C). Measurements of the signal intensity change of a constant signal pattern further demonstrated that the product formation proceeded in a processive manner with no free RNA intermediates detectable. In these experiments, 20 $\mu$M polymerase−3′(−)SL RNA complex was applied to the assay. Considering this value, the ternary complex decay and product release in a single turnover reaction was estimated to proceed with a $k_{cat} \approx 0.1$ min$^{-1}$ with regard to NTPs.

## DISCUSSION

**HCV-Polymerase Binding of the RNA Template.** About a decade ago, the structure elucidation of the HCV-polymerase led to the assumption that substrate/template binding and double-stranded RNA product formation are necessarily accommodated by major conformational changes of the enzyme to an open conformation.[13,14] This view was supported by a recent report of Rigat et al.[30] These authors demonstrated that in solution and while binding RNA an otherwise

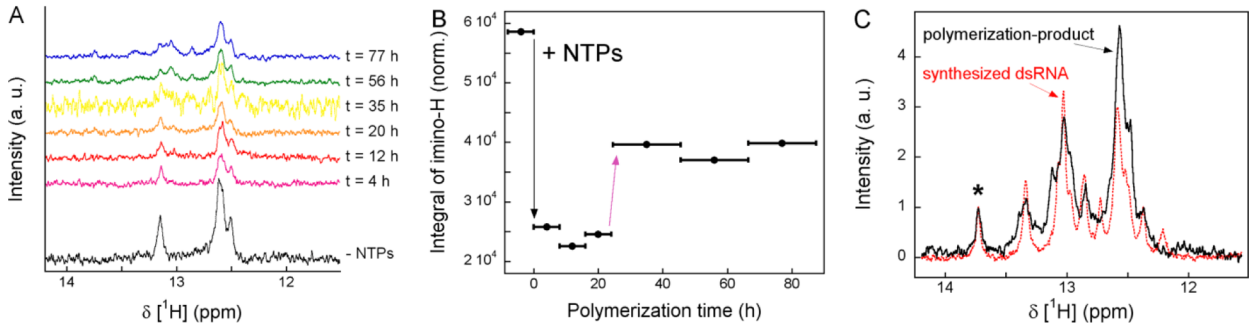


**Figure 6.** RNA-dependent RNA polymerization monitored by real-time 1D $^1$H NMR spectroscopy. Product formation (double-stranded RNA) by the HCV-polymerase was monitored with the native 3′(−)SL RNA template following the addition of NTPs. (A) Proton spectra sensing double-stranded RNA were recorded at different time points of the polymerization reaction: 0−8 h, magenta; 8−16 h, red; 16−24 h, orange; 25−46 h, yellow; 46−67 h, green; and 67−88 h, blue after the addition of NTP to the polymerase−RNA complex (binary complex) (black). Upon binding of NTPs to the binary complex, the intensity of the RNA-related $^1$H NMR signals decreased. During an initial period of ca. 24 h, a constant signal pattern of the RNA was observed. After about 25 h, newly developed imino proton NMR signals were detectable that corresponded to the released double-stranded RNA product. (B) The enzymatic progress curve illustrates the HCV-polymerase interacting with the partially double-stranded 3′(−)SL RNA as well as the subsequent product formation and release process of the double-stranded RNA. The initial decrease of the integrated imino proton NMR signals upon addition of NTPs indicates an increased affinity for the RNA template in the catalysis-competent ternary complex compared to the binary polymerase−RNA complex. After a significant lag phase, new imino proton NMR signals developed, corresponding to dsRNA product formation and release. The $k_{cat} \approx 0.1$ min$^{-1}$ (NTP) was determined assuming that 20 $\mu$M RNA product (21 bp) was produced by 20 $\mu$M polymerase−RNA complex within 5 h. The horizontal bars reflect the time of accumulation of the respective spectra. (C) Comparison of the 1D $^1$H NMR spectrum of the product of the HCV-polymerase-catalyzed polymerization reaction (solid black line) with a chemically synthesized and annealed 21 bp double-stranded RNA (dashed red line). The integral of the signal at 13.75 ppm in the $^1$H NMR spectrum (marked by an asterisk) is equal to 0.05 of the total integral of all imino proton signals, as expected for 21 paired bases.


dx.doi.org/10.1021/bi5006656 | Biochemistry 2014, 53, 7002−7012

compacted region of the polymerase becomes hypersensitive to proteolysis. Consistently, our kinetic and thermodynamic studies suggest that the HCV-polymerase adopts different conformations while interacting with the template. Both the randomly composed single-stranded RNA as well as the structured 3′(−)SL RNA were shown to interact with the HCV-polymerase, although with different affinities. Kinetically, these differences were realized by the second-order rate constant of association. Following the formation of the very initial polymerase−RNA complex, additional steps were monitored that occurred independently of the RNA concentration and RNA moiety and most likely reflect conformational transitions of the polymerase. The here-applied fluorescence-based assay enabled accurate measurements of the affinity constants of the HCV-polymerase and the RNAs and revealed that the formation of the binary polymerase−RNA complex follows a linear free energy relationship that typically governs chemical processes. The finding that the Gibbs free binding energy is differently perturbed in dependence on the nature of the RNA template accordingly suggests that the HCV-polymerase is capable to adapt to differently structured RNAs and to realize various binding modes. Interestingly, the distinction of templates by the polymerase manifests during the very initial interaction rather than in the course of subsequent intramolecular positioning reactions. This fuels the speculation that different subpopulations of the native state of RNAs may be bound by slightly differing sets of residues on the enzyme's surface. van't Hoff analysis of the polymerase−RNA interaction demonstrated that the binding of RNA by the polymerase is generally entropically driven. Compared to the situation with the ssRNA, the association of the structured 3′(−)SL RNA even increased favorable entropic contributions. Since the interaction of the polymerase with the 3′(−)SL RNA turned out to be also less dependent on the ionic strength compared to ssRNA, we explained this increase of entropy not only by solvation effects but also by an increase of the conformational freedom of this polymerase−RNA complex. Considering that unfavorable enthalpic contributions usually arise by the disruption of existing interactions, this data further supports earlier studies that binary complex formation requires an opening of the HCV-polymerase.[7,9,10,14,17,22,23,30−32]

**Formation of the Catalysis-Competent Ternary Complex.** Upon the binding of NTPs and RNA template, the polymerase forms the catalysis-competent ternary complex, which also involves a selection mechanism to incorporate the cognate nucleotide into the growing dsRNA product. Like many, if not all, template-directed polymerases, this process is accompanied by conformational rearrangements of some closed states back to some open or ajar states, where improper nucleotides might exit the active site prior to misincorporation.[33,34] Our experimental setup allowed the quantification of the interaction of NTPs with the polymerase in the absence of RNA template. Two NTP molecules were shown to bind to the HCV-polymerase with positive cooperativity at dissociation constants in the micromolar range (Table 4). This indicated that one NTP associates with the nucleotide binding site while the second NTP, due to its chemical similarity with the RNA template, presumably interacts with the RNA binding site. To show the impact of nucleotides on the RNA-loaded HCV-polymerase, we monitored the imino proton signals of the 3′(−)SL RNA in the presence of the HCV-polymerase by NMR spectroscopy. Note that the 1D $^1$H NMR spectrum of the binary complex containing the 3′(−)SL RNA reflects only the unbound nucleic acid that is in equilibrium with the enzyme. Following the addition of nucleotides, the NMR signals of the imino protons of the RNA template decreased rapidly, indicating a decrease in the concentration of the unbound RNA. This data demonstrated an increase of the template's affinity in forming the catalysis-competent ternary complex (see 4 h spectrum in Figure 6A,B). Hence, the association of NTPs resulted in a positive cooperative binding of the RNA template. A structural rearrangement of the HCV-polymerase was also monitored by circular dichroism as the protein's ellipticity changed after the addition of NTPs (Supporting Information Figure S1).

**Double-Stranded RNA Product Formation and Release.** Previous studies demonstrated that the purified HCV-polymerase is capable of *de novo* initiation of RNA polymerization.[5,6] Accordingly, for the synthesis of progeny (+)RNA molecules in the HCV replication process, initiation essentially occurs at the immediate 3′-end of the (−)RNA to prohibit the loss of genetic information. As demonstrated here by $^1$H NMR spectroscopy, the applied 3′(−)SL RNA that corresponds to the HCV (−)RNA's 3′-end adopts stable stem-loop structures. Signal changes in the RNA's 1D $^1$H NMR spectra during polymerization revealed the formation of the final double-stranded RNA product in real time when the reaction was started by the addition of NTPs. A 21 bp product was detected, indicating that a (+)RNA molecule was synthesized by *de novo* initiation that was full-length complementary to the 3′(−)SL template. Interestingly, with the structured 3′(−)SL RNA template, we observed an evident lag phase that preceded product formation (Figure 6B). This was in contrast to observations during earlier experiments that applied a non-structured ssRNA as a template.[28] It was also unexpected because conventional radioactive assay systems commonly detect *de novo* RNA synthesis by the HCV-polymerase within minutes to hours.[16,35] One explanation for this discrepancy may relate to the short 3′(−)SL template that was applied here on purpose to specifically investigate the polymerase's activity on a highly homogeneous and structured template. The conventional assays mostly applied long RNA transcripts and thus contained populations of various RNA conformations, some of which may be immediately susceptible to polymerization. Another explanation relates to the NMR assay, which, in contrast to a radioactive incorporation assay, focuses exclusively on the detection of the predominant product. In any case, the apparent delay in product formation with the 3′(−)SL template clearly points to the requirement of an additional mechanism of activation that makes this template more susceptible to efficient polymerization (see below).

How does the polymerase deal with the 3′(−)SL RNA? Temperature transitions with the unbound RNA demonstrated that the stem's edge base pair $G_3$−$C_{17}$ is thermodynamically more stable than the intrinsic base pairs. This indicated local differences in the intramolecular stability of the RNA structures and suggests that the folding/unfolding of the stem proceeds consecutively ("breathing"). Initiation of RNA synthesis by the polymerase thus requires first an opening of the edge base pair $G_3$−$C_{17}$, which would then result in a destabilization of the whole stem. In the course of the enzymatic polymerization reaction, the entire stem-loop RNA structure is accordingly expected to cooperatively unfold by coupling to binding,[36] with the edge base pair $G_3$−$C_{17}$ being the main energy barrier. Concerning the enzymatic characteristics of the HCV-polymerase, it is important to note that almost all two-substrate-two-


dx.doi.org/10.1021/bi5006656 | *Biochemistry* 2014, 53, 7002−7012

product reactions such as nucleotidyl-transfer are formally group-transfer reactions.[37] They are further mechanistically classified according to their sequence in turnover (i.e., substrate binding and product release). Regarding the experimentally identified two half-reactions of substrate binding by the HCV-polymerase, namely, of the RNA template and NTPs, the entire enzymatic reaction can be termed to proceed according to a random-order ternary complex mechanism. This mechanism is characterized by a random binding of the two substrates that form individual binary complexes and that finally result in ternary complex formation. During the entire polymerization reaction, the inorganic diphosphate product will release from the ternary complex, thus yielding another defined binary complex that contains the bound polymer substrate ready for the subsequent second half-reaction (next nucleotide incorporation). As the polymerization product is a double-stranded RNA, binding of the stem-containing 3′(−)SL RNA template will at least partially result in a more product-like state. This notion is in line with the finding that the polymerase binds ssRNA with a significantly higher affinity (smaller $K_D$ value). An enzyme-bound single-stranded template RNA is accordingly expected to be more accessible for nucleotide incorporation and supposed to be stabilized intramolecularly. In turn, this implies that the incorporation of NTPs requires an unfolding of the 3′(−)SL RNA secondary structure. Besides monitoring substrate binding and product release, our data does not provide detailed information about conformational changes of the enzyme-bound substrates or products. Since no free product-like intermediates were detectable (Figure 6), the NMR experiments clearly revealed the processive action of the HCV-polymerase. However, with the 3′(−)SL template, the rate constant $k_{cat}$ was only 0.1 $min^{-1}$. This was in contrast with nonstructured RNA, where $k_{cat}$ was bigger than 10 $min^{-1}$[35] and indicates an impaired activity of the polymerase on the structured RNA. Moreover, these observations suggest that NS5B has no significant helicase activity that would enable the enzyme to destabilize the double-stranded moiety of 3′(−)SL and effectively initiate RNA synthesis also on this template. While the NS5B RdRp catalyzes the amplification of the HCV genome, an as yet uncertain number of supporting viral and host factors are implicated to assist this process (for review, see ref 1). This report accordingly highlights the potential role of RNA helicases, RNA chaperones, or RNA annealers that are expected to either directly affect the sequential enzymatic action of NS5B and/or to modulate the active structure of the RNA template. The here established techniques are expected to considerably guide the further characterization of the function of, for example, the viral helicase NS3 or cell-encoded RNA binding proteins that were indicated to support HCV replication.[38−43]

## ■ ASSOCIATED CONTENT

### Supporting Information

NTP binding parameters to the HCV-polymerase and protocols for enzyme purification and for measuring RNA binding to the enzyme by stopped-flow kinetics. This material is available free of charge via the Internet at http://pubs.acs.org.

## ■ AUTHOR INFORMATION


### Corresponding Authors

*(R.P.G.) E-mail: golbik@biochemtech.uni-halle.de. Tel.: +49-3455524912. Fax: +49-3455527387.

*(S.-E.B.) E-mail: behrens@biochemtech.uni-halle.de.


### Author Contributions

Stefan Reich designed and performed experiments and wrote the manuscript. Michael Kovermann performed experiments. Hauke Lilie performed experiments. Paul Knick performed experiments. Rene Geissler performed experiments. Ralph Peter Golbik, Jochen Balbach, and Sven-Erik Behrens designed experiments and wrote the manuscript.


### Funding

The project was supported by the National Institutes of Health (grant no. 5-RO1-DK-62847-3 to S.-E.B.), by the Deutsche Forschungsgemeinschaft (grant nos. BE 1885/6-1 and 1885/6-2 to R.G. and P.K., and grants from the SFB 610 to M.K.), by the Graduiertenkolleg 1026 (grants to S.R. and M.K.), and by the Exzellenzinitiative of the State of Saxony-Anhalt.


### Notes

The authors declare no competing financial interest.

## ■ ACKNOWLEDGMENTS


Significant investments into our NMR facility from the European Regional Development Fund (ERDF) by the European Union are gratefully acknowledged.


## ■ ABBREVIATIONS

bp, base pair(s); 5′-FAM-EX-5, 6-carboxy-fluoresceine attached to the 5′-end of RNA; JFH, Japanese fulminant hepatitis; LFER, linear free energy relationship; NS5B, nonstructural protein 5B; NTP(s)/nt, nucleotide(s); SL, stem loop; ssRNA, single-stranded RNA

## ■ REFERENCES


(1) Lindenbach, B. D., Thiel, H. J., and Rice, C. M. (2007) *Flaviviridae*: the viruses and their replication, in *Fields Virology* (Knipe, D. M., and Howley, P. M., Eds.) 5th ed., pp 1101−1152, Lippincott-Raven Publishers, Philadelphia, PA.

(2) Bartenschlager, R., and Lohmann, V. (2000) Replication of hepatitis C virus. *J. Gen. Virol. 81*, 1631−1648.

(3) Behrens, S. E., Tomei, L., and De Francesco, R. (1996) Identification and properties of the RNA-dependent RNA polymerase of hepatitis C virus. *EMBO J. 15*, 12−22.

(4) Lohmann, V., Korner, F., Herian, U., and Bartenschlager, R. (1997) Biochemical properties of hepatitis C virus NS5B RNA-dependent RNA polymerase and identification of amino acid sequence motifs essential for enzymatic activity. *J. Virol. 71*, 8416−8428.

(5) Oh, J. W., Ito, T., and Lai, M. M. (1999) A recombinant hepatitis C virus RNA-dependent RNA polymerase capable of copying the full-length viral RNA. *J. Virol. 73*, 7694−7702.

(6) Luo, G., Hamatake, R. K., Mathis, D. M., Racela, J., Rigat, K. L., Lemm, J., and Colonno, R. J. (2000) *De novo* initiation of RNA synthesis by the RNA-dependent RNA polymerase (NS5B) of hepatitis C virus. *J. Virol. 74*, 851−863.

(7) Wang, M., Ng, K. K., Cherney, M. M., Chan, L., Yannopoulos, C. G., Bedard, J., Morin, N., Nguyen-Ba, N., Alaoui-Ismaili, M. H., Bethell, R. C., and James, M. N. (2003) Non-nucleoside analogue inhibitors bind to an allosteric site on HCV NS5B polymerase. Crystal structures and mechanism of inhibition. *J. Biol. Chem. 278*, 9489−9495.

(8) Chinnaswamy, S., Murali, A., Li, P., Fujisaki, K., and Kao, C. C. (2010) Regulation of *de novo*-initiated RNA synthesis in hepatitis C virus RNA-dependent RNA polymerase by intermolecular interactions. *J. Virol. 84*, 5923−5935.

(9) Di Marco, S., Volpari, C., Tomei, L., Altamura, S., Harper, S., Narjes, F., Koch, U., Rowley, M., De Francesco, R., Migliaccio, G., and Carfi, A. (2005) Interdomain communication in hepatitis C virus polymerase abolished by small molecule inhibitors bound to a novel allosteric site. *J. Biol. Chem. 280*, 29765−29770.

(10) Liu, Y., Jiang, W. W., Pratt, J., Rockway, T., Harris, K., Vasavanonda, S., Tripathi, R., Pithawalla, R., and Kati, W. M. (2006) Mechanistic study of HCV polymerase inhibitors at individual steps of the polymerization reaction. *Biochemistry 45*, 11312−11323.
(11) Betzi, S., Eydoux, C., Bussetta, C., Blemont, M., Leyssen, P., Debarnot, C., Ben-Rahou, M., Haiech, J., Hibert, M., Gueritte, F., Grierson, D. S., Romette, J. L., Guillemot, J. C., Neyts, J., Alvarez, K., Morelli, X., Dutartre, H., and Canard, B. (2009) Identification of allosteric inhibitors blocking the hepatitis C virus polymerase NS5B in the RNA synthesis initiation step. *Antiviral Res. 84*, 48−59.
(12) Ferrari, E., He, Z., Palermo, R. E., and Huang, H. C. (2008) Hepatitis C virus NS5B polymerase exhibits distinct nucleotide requirements for initiation and elongation. *J. Biol. Chem. 283*, 33893−33901.
(13) Ago, H., Adachi, T., Yoshida, A., Yamamoto, M., Habuka, N., Yatsunami, K., and Miyano, M. (1999) Crystal structure of the RNA-dependent RNA polymerase of hepatitis C virus. *Structure 7*, 1417−1426.
(14) Bressanelli, S., Tomei, L., Roussel, A., Incitti, I., Vitale, R. L., Mathieu, M., De Francesco, R., and Rey, F. A. (1999) Crystal structure of the RNA-dependent RNA polymerase of hepatitis C virus. *Proc. Natl. Acad. Sci. U.S.A. 96*, 13034−13039.
(15) Lesburg, C. A., Cable, M. B., Ferrari, E., Hong, Z., Mannarino, A. F., and Weber, P. C. (1999) Crystal structure of the RNA-dependent RNA polymerase from hepatitis C virus reveals a fully encircled active site. *Nat. Struct. Biol. 6*, 937−943.
(16) Simister, P., Schmitt, M., Geitmann, M., Wicht, O., Danielson, U. H., Klein, R., Bressanelli, S., and Lohmann, V. (2009) Structural and functional analysis of hepatitis C virus strain JFH1 polymerase. *J. Virol. 83*, 11926−11939.
(17) Harrus, D., Ahmed-El-Sayed, N., Simister, P. C., Miller, S., Triconnet, M., Hagedorn, C. H., Mahias, K., Rey, F. A., Astier-Gin, T., and Bressanelli, S. (2010) Further insights into the roles of GTP and the C terminus of the hepatitis C virus polymerase in the initiation of RNA synthesis. *J. Biol. Chem. 285*, 32906−32918.
(18) Labonte, P., Axelrod, V., Agarwal, A., Aulabaugh, A., Amin, A., and Mak, P. (2002) Modulation of hepatitis C virus RNA-dependent RNA polymerase activity by structure-based site-directed mutagenesis. *J. Biol. Chem. 277*, 38838−38846.
(19) Kim, Y. C., Russell, W. K., Ranjith-Kumar, C. T., Thomson, M., Russell, D. H., and Kao, C. C. (2005) Functional analysis of RNA binding by the hepatitis C virus RNA-dependent RNA polymerase. *J. Biol. Chem. 280*, 38011−38019.
(20) Adachi, T., Ago, H., Habuka, N., Okuda, K., Komatsu, M., Ikeda, S., and Yatsunami, K. (2002) The essential role of C-terminal residues in regulating the activity of hepatitis C virus RNA-dependent RNA polymerase. *Biochim. Biophys. Acta 1601*, 38−48.
(21) Ranjith-Kumar, C. T., Gutshall, L., Sarisky, R. T., and Kao, C. C. (2003) Multiple interactions within the hepatitis C virus RNA polymerase repress primer-dependent RNA synthesis. *J. Mol. Biol. 330*, 675−685.
(22) Ranjith-Kumar, C. T., and Kao, C. C. (2006) Recombinant viral RdRps can initiate RNA synthesis from circular templates. *RNA 12*, 303−312.
(23) Biswal, B. K., Cherney, M. M., Wang, M., Chan, L., Yannopoulos, C. G., Bilimoria, D., Nicolas, O., Bedard, J., and James, M. N. (2005) Crystal structures of the RNA-dependent RNA polymerase genotype 2a of hepatitis C virus reveal two conformations and suggest mechanisms of inhibition by non-nucleoside inhibitors. *J. Biol. Chem. 280*, 18202−18210.
(24) Biswal, B. K., Wang, M., Cherney, M. M., Chan, L., Yannopoulos, C. G., Bilimoria, D., Bedard, J., and James, M. N. (2006) Non-nucleoside inhibitors binding to hepatitis C virus NS5B polymerase reveal a novel mechanism of inhibition. *J. Mol. Biol. 361*, 33−45.
(25) Cameron, C. E., Moustafa, I. M., and Arnold, J. J. (2009) Dynamics: the missing link between structure and function of the viral RNA-dependent RNA polymerase? *Curr. Opin. Struct. Biol. 19*, 768−774.
(26) Balbach, J., Forge, V., van Nuland, N. A., Winder, S. L., Hore, P. J., and Dobson, C. M. (1995) Following protein folding in real time using NMR spectroscopy. *Nat. Struct. Biol. 2*, 865−870.
(27) Zeeb, M., and Balbach, J. (2004) Protein folding studied by real-time NMR spectroscopy. *Methods 34*, 65−74.
(28) Reich, S., Golbik, R. P., Geissler, R., Lilie, H., and Behrens, S. E. (2010) Mechanisms of activity and inhibition of the hepatitis C virus RNA-dependent RNA polymerase. *J. Biol. Chem. 285*, 13685−13693.
(29) Rinnenthal, J., Klinkert, B., Narberhaus, F., and Schwalbe, H. (2010) Direct observation of the temperature-induced melting process of the Salmonella fourU RNA thermometer at base-pair resolution. *Nucleic Acids Res. 38*, 3834−3847.
(30) Rigat, K., Wang, Y., Hudyma, T. W., Ding, M., Zheng, X., Gentles, R. G., Beno, B. R., Gao, M., and Roberts, S. B. (2010) Ligand-induced changes in hepatitis C virus NS5B polymerase structure. *Antiviral Res. 88*, 197−206.
(31) Hong, Z., Cameron, C. E., Walker, M. P., Castro, C., Yao, N., Lau, J. Y., and Zhong, W. (2001) A novel mechanism to ensure terminal initiation by hepatitis C virus NS5B polymerase. *Virology 285*, 6−11.
(32) Howe, A. Y., Cheng, H., Thompson, I., Chunduru, S. K., Herrmann, S., O'Connell, J., Agarwal, A., Chopra, R., and Del Vecchio, A. M. (2006) Molecular mechanism of a thumb domain hepatitis C virus nonnucleoside RNA-dependent RNA polymerase inhibitor. *Antimicrob. Agents Chemother. 50*, 4103−4113.
(33) Wu, E. Y., and Beese, L. S. (2011) The structure of a high fidelity DNA polymerase bound to a mismatched nucleotide reveals an "ajar" intermediate conformation in the nucleotide selection mechanism. *J. Biol. Chem. 286*, 19758−19767.
(34) Tsai, Y. C., and Johnson, K. A. (2006) A new paradigm for DNA polymerase specificity. *Biochemistry 45*, 9675−9687.
(35) Jin, Z., Leveque, V., Ma, H., Johnson, K. A., and Klumpp, K. (2012) Assembly, purification, and pre-steady-state kinetic analysis of active RNA-dependent RNA polymerase elongation complex. *J. Biol. Chem. 287*, 10674−10683.
(36) Kiefhaber, T., Bachmann, A., and Jensen, K. S. (2012) Dynamics and mechanisms of coupled protein folding and binding reactions. *Curr. Opin. Struct. Biol. 22*, 21−29.
(37) Cornish-Bowden, A. (2012) *Fundamentals of Enzyme Kinetics*, 4th ed. ed., Wiley-VCH Verlag & Co. KGaA, Weinheim, Germany.
(38) Isken, O., Baroth, M., Grassmann, C. W., Weinlich, S., Ostareck, D. H., Ostareck-Lederer, A., and Behrens, S. E. (2007) Nuclear factors are involved in hepatitis C virus RNA replication. *RNA 13*, 1675−1692.
(39) Piccininni, S., Varaklioti, A., Nardelli, M., Dave, B., Raney, K. D., and McCarthy, J. E. (2002) Modulation of the hepatitis C virus RNA-dependent RNA polymerase activity by the non-structural (NS) 3 helicase and the NS4B membrane protein. *J. Biol. Chem. 277*, 45670−45679.
(40) Chinnaswamy, S., Yarbrough, I., Palaninathan, S., Kumar, C. T., Vijayaraghavan, V., Demeler, B., Lemon, S. M., Sacchettini, J. C., and Kao, C. C. (2008) A locking mechanism regulates RNA synthesis and host protein interaction by the hepatitis C virus polymerase. *J. Biol. Chem. 283*, 20535−20546.
(41) Inoue, Y., Aizaki, H., Hara, H., Matsuda, M., Ando, T., Shimoji, T., Murakami, K., Masaki, T., Shoji, I., Homma, S., Matsuura, Y., Miyamura, T., Wakita, T., and Suzuki, T. (2011) Chaperonin TRiC/CCT participates in replication of hepatitis C virus genome via interaction with the viral NS5B protein. *Virology 410*, 38−47.
(42) Ng, T. I., Mo, H., Pilot-Matias, T., He, Y., Koev, G., Krishnan, P., Mondal, R., Pithawalla, R., He, W., Dekhtyar, T., Packer, J., Schurdak, M., and Molla, A. (2007) Identification of host genes involved in hepatitis C virus replication by small interfering RNA technology. *Hepatology 45*, 1413−1421.
(43) Goh, P. Y., Tan, Y. J., Lim, S. P., Tan, Y. H., Lim, S. G., Fuller-Pace, F., and Hong, W. (2004) Cellular RNA helicase p68 relocalization and interaction with the hepatitis C virus (HCV) NS5B protein and the potential role of p68 in HCV RNA replication. *J. Virol. 78*, 5288−5298.

(44) Hwang, T. H., and Shaka, A. J. (1995) Water suppression that works. Excitation sculpting using arbitrary waveforms and pulsed field gradients. *J. Magn. Reson., Ser. A 112*, 275−279.
(45) Zuker, M. (2003) Mfold web server for nucleic acid folding and hybridization prediction. *Nucleic Acids Res. 31*, 3406−3415.
(46) Wells, T. N., and Fersht, A. R. (1989) Protection of an unstable reaction intermediate examined with linear free energy relationships in tyrosyl-tRNA synthetase. *Biochemistry 28*, 9201−9209.
(47) Fersht, A. R., Leatherbarrow, R. J., and Wells, T. N. (1987) Structure−activity relationships in engineered proteins: analysis of use of binding energy by linear free energy relationships. *Biochemistry 26*, 6030−6038.